

Anhyseretic Magnetization for NiFeMo Soft Magnetic Compacted Powder

D. OLEKŠÁKOVÁ^{a,*}, P. KOLLÁR^b, M. JAKUBČIN^b, P. SLOVENSKÝ^b,
Z. BIRČÁKOVÁ^c, J. FÜZER^b, M. FÁBEROVÁ^c AND R. BUREŠ^c

^aInstitute of Manufacturing Management, Faculty of Manufacturing Technologies with the seat in Prešov,
Technical University of Košice, Bayerova 1, 080 01 Prešov, Slovakia

^bInstitute of Physics, Faculty of Science, P.J. Šafárik University, Park Angelinum 9, 041 54 Košice, Slovakia

^cInstitute of Materials Research, Slovak Academy of Sciences, Watsonova 47, 043 53 Košice, Slovakia

Experimentally obtained anhyseretic curves, which characterize NiFeMo soft magnetic compacted powders were measured by modified DC hysteresisgraph. Two anhyseretic curves of two properly prepared samples were compared. First sample was compacted from powder obtained by milling of small chips with particle size between 100 μm and 300 μm . Then, the surface particles were mechanically smoothed. Second sample was prepared in the same way as first one, only that after compaction the sample was annealed at 1100 °C. Numerical analysis of anhyseretic curves showed that the origin of the improvement of the soft magnetic properties of the bulk is due to annealing.

DOI: [10.12693/APhysPolA.137.889](https://doi.org/10.12693/APhysPolA.137.889)

PACS/topics: soft magnetic material, anhyseretic curve, demagnetization factor

1. Introduction

Nickel iron alloys (permalloys) are important in many areas of science from material research and engineering [1] to the planetary sciences (founded in most meteorite classes) [2]. High permeability and low magnetostrictive properties of permalloys are widely used in magnetic cores for electrical equipment applications. They are also useful as magnetic shielding materials [3]. Nickel iron alloys are still attractive systems to study because their applications being one of the primary concerns in science and technology of materials [4, 5].

In the present work, we study Ni-rich Mo substituted permalloys. Generally, Mo enhances material permeability even if a small amount is added [6]. High permeability can be also achieved by reducing the amount of Ni. In turn, Mo increases the electrical resistivity of permalloys, and reduces eddy current losses at the same time. Iron nickel molybdenum alloys (called supermalloy) show excellent high frequency characteristics [6, 7].

The appropriate structure of the supermalloy (produced usually in the form of thin sheet) with initial permeability much larger than that of pure iron arises after proper heat treatment. For some applications the form of a sheet is not suitable, therefore it is logical to try to prepare such material in another form, for example in a form of a ring. This shape would be more convenient for construction of some type components for electronic devices [6]. One of the methods of preparing 3D samples is the compaction of powder obtained by the mechanical milling, or mechanical alloying [8].

In this paper, we demonstrate the matching to the anhyseretic curve of experimental data for compacted Ni₈₀Fe₁₅Mo₅ (wt. %) based on the Jiles-Atherton model with an additional parameter. The influence of annealing on parameters from the Jiles-Atherton model is also examined.

2. Experimental

Small chips Ni₈₀Fe₁₅Mo₅ (wt. %) with size of 2 mm were prepared from the sheet by a rotary drill grinder mounted in a lathe. The chips were milled in a planetary ball mill Retch PM100 in steel vial with steel balls for 10 min with BPR ratio 10:1. The morphology of the chips and the milled chips (powder) was scanned by optical microscope (Nikon Epiphot 200), and scanning electron microscope (TESCAN VEGA3), displayed in Fig. 1. The milled powder was sieved to obtain size fraction from 100 μm to 300 μm . The powder particles were mechanically smoothed [9], and compacted by uniaxial pressure of 700 MPa at the temperature of 410 °C with durability of 10 min, sample A. The B sample was prepared by the same way, only after compaction the sample was annealed at 1100 °C for 10 hours in hydrogen atmosphere. The dimensions of resulted bulk samples were: height of 2.9 mm, outer diameter of 24 mm, and inner diameter of 18 mm. The detailed samples parameters including density are given in [9].

3. Anhyseretic curves

The anhyseretic magnetization curve (also called “ideal magnetization” [10]) is a concept used extensively in the characterization of magnetic materials. Anhyseretic magnetization is defined as the “thermal equilibrium” curve measured by the cooling the sample from

*corresponding author; e-mail: denisa.oleksakova@tuke.sk

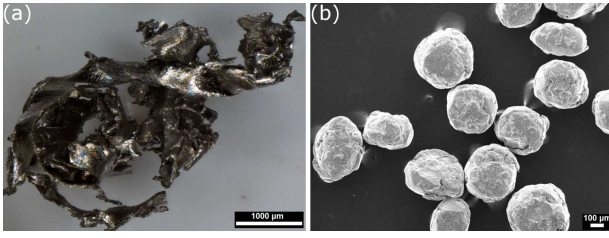


Fig. 1. The morphology (a) of the chips $\text{Ni}_{80}\text{Fe}_{15}\text{Mo}_5$ (wt%), visualized by optical microscope, and (b) the powdered chips, which powder element were mechanically smoothed $\text{Ni}_{80}\text{Fe}_{15}\text{Mo}_5$ (wt%) visualized by SEM.

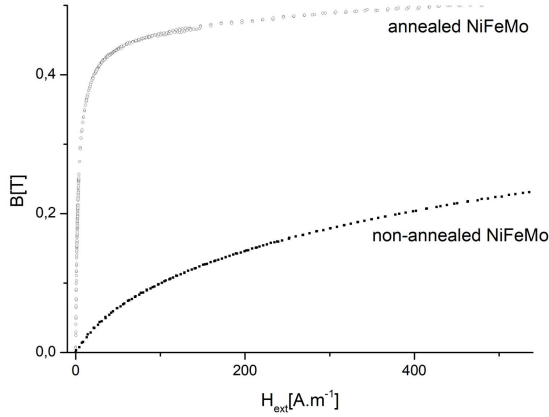


Fig. 2. Anhyseretic curves of compacted $\text{Ni}_{80}\text{Fe}_{15}\text{Mo}_5$ (wt%) before the annealing and after the annealing at $1100\text{ }^\circ\text{C}$.

the Curie temperature in an incrementally increased direct current DC field [11, 12]. The most important utilization of anhyseretic curves is in magnetic recording, where the superposition of high frequency field (also called “bias”) on the signal is used to overcome the hysteresis of the recording medium [12].

Anhyseretic curves (Fig. 2) were measured by modified DC hysteresisgraph. The AC field with decreased amplitude was applied at every measured point along the magnetization curve by the third toroidal winding to obtain experimental points of anhyseretic curve [13, 14]. In the figure there are the values of external magnetic field H_{ext} (produced by third windings on ring-shaped sample) on x-axis.

4. Inner demagnetization factor

Since the samples used for measurements were prepared by compaction of powder, then each powder element as a source of demagnetizing field reduces the value of internal magnetic field H_{int} . It is expressed as follows:

$$H_{\text{int}} = H_{\text{ext}} - H_d = H_{\text{ext}} - N_d M, \quad (1)$$

where H_d is demagnetization field, N_d is inner demagnetization factor, and M is the magnetization.

TABLE I

Calculated (dimensionless) coefficients of compacted $\text{Ni}_{80}\text{Fe}_{15}\text{Mo}_5$ (wt %) before the annealing and after the annealing at $1100\text{ }^\circ\text{C}$.

Coefficient	Before the annealing	After the annealing
N_d [-]	6.69×10^{-4}	3.14×10^{-6}
K_1 [m/A]	94×10^{-4}	10.385×10^{-4}
K_2 [m/A]	5.07×10^{-6}	6.295×10^{-6}
m [A/m]	3049.36×10^{-10}	336.89×10^{-10}
α [-]	53.94×10^{-3}	6.06×10^{-3}

The demagnetization factor was determined by the linear part of anhyseretic curve for $H_{\text{ext}} \rightarrow 0$. Demagnetization field in the sample depends on numerous parameters, such as shape and size of particles, and porosity [13]. To determine the demagnetization factor one can use formula [13]

$$N_d = \left(\frac{B}{\mu_0 H_{\text{ext}}} - 1 \right)^{-1}, \quad (2)$$

where B is the magnetic induction, and B/H_{ext} is the slope of the linear part of anhyseretic curve. The values of demagnetization factor of compacted $\text{Ni}_{80}\text{Fe}_{15}\text{Mo}_5$ (wt%), before the annealing and after the annealing at $1100\text{ }^\circ\text{C}$, are in Table I. The value of the demagnetization factor for annealed sample is significantly lower than that for non-annealed sample due to the paths creation between powder elements for magnetic induction.

5. Jiles-Atherton model

Nowadays, the anhyseretic magnetization curves are often processed with the Jiles-Atherton model of magnetic hysteresis [15]. This one of most popular magnetic models is suitable for design and simulations of electrotechnical and electronic components with soft magnetic cores [16]. The model itself is based on the anhyseretic curves, which are derived using a mean field approach, and where the magnetization of any domain is coupled to the magnetic field H_{int} and the bulk magnetization M [15, 17].

According to Jiles-Atherton model [15] the energy E of a domain with the magnetic moment m of ferromagnetic material in the presence of the magnetic field H_{int} is:

$$E = \mu_0 m H_E = \mu_0 m (H_I + H_{\text{int}}), \quad (3)$$

where μ_0 is permeability of vacuum, H_E is the effective magnetic field, and H_I is the magnetic field representing inter domain coupling. Typically, H_I determines the shape of the anhyseretic magnetic curve, and according to the Jiles-Atherton model [15] it is

$$H_I = f(M), \quad H_I(M) = \alpha M, \quad \alpha = \alpha(M), \quad (4)$$

where α is a constant mean field parameter. Now, (3) can be rewritten as

$$E = \mu_0 m (\alpha M + H_{\text{int}}). \quad (5)$$

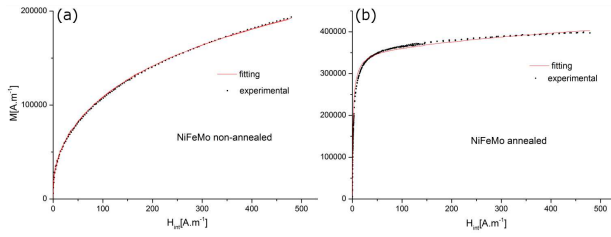


Fig. 3. Anhyseresis curves and calculated ones for fitted parameters m , α in Langevin function of $\text{Ni}_{80}\text{Fe}_{15}\text{Mo}_5$ compacts before the annealing (a) and after the annealing (b) at $1100\text{ }^\circ\text{C}$.

According to the Jiles-Atherton model, which is based on the idea of anhyseretic magnetization M of ferromagnetic material, after applying Maxwell-Boltzman statistics (distribution of magnetization vectors of domains) and introducing the modified Langevin function \mathcal{L} , we can write:

$$M = M_s \mathcal{L} \left(\frac{E}{k_B T} \right) = M_s \mathcal{L} \left(\frac{\mu_0 m}{k_B T} (\alpha M + H_{\text{int}}) \right)$$

$$K_1 = \frac{\mu_0 m}{k_B T}, \quad K_2 = K_1 \alpha, \quad (6)$$

$$M = M_s (K_1 H_{\text{int}} + K_2 M), \quad (7)$$

where k_B is Boltzmann constant, M_s is the saturation magnetization, and K_1 , K_2 are parameters, which can be fitted according to (7) based on experimental data of anhyseretic curves for two compacted $\text{Ni}_{80}\text{Fe}_{15}\text{Mo}_5$ samples (wt%) before the annealing and after the annealing at $1100\text{ }^\circ\text{C}$. Parameter K_1 depends on the room temperature T , and the average magnetic moment of an effective domain m . Definition of K_1 includes the Boltzmann constant k_B , as well as the magnetic constant μ_0 . Parameter K_2 is consistent with a constant mean field parameter α in (4).

The fitted parameters K_1 , K_2 , and calculated parameters m , α can be found in Table I. The values of m are unexpectedly low, which is explained in [18]. The comparison between measured anhyseretic curves for both samples with theoretical ones obtained with m and α parameters, is depicted in Fig. 3.

5. Conclusions

Experimental data of anhyseretic curves (before the annealing and after the annealing at $1100\text{ }^\circ\text{C}$) of the compacted powder $\text{Ni}_{80}\text{Fe}_{15}\text{Mo}_5$ sample with particle size from $100\text{ }\mu\text{m}$ to $300\text{ }\mu\text{m}$, were compared with Jiles-Atherton model for ferromagnetic material. At first, however, the parameters of Langevin function were determined. The annealing causes a significant decrease of the parameter m (the average magnetic moment of an effective domain), and a slight decrease of the parameter α (the mean field parameter). It is treated as a consequence of the creation of the paths for magnetic flux between powder elements in the compacted material.

The decrease of parameters values leads to stronger coupling, and denser effective domains after annealing. We can summarize that the presented model matches the experimental data with very good accuracy.

Acknowledgments

This work was financed by Scientific Grant Agency of Ministry of Education of Slovak Republic and Slovak Academy of Science — projects VEGA 1/0301/20, VEGA 1/0143/20 and KEGA 002TUKE-4/2019. This work was also supported by the Development Operational Programme Research and Innovation for the project “New unconventional magnetic materials for applications”, ITMS: 313011T544, co-funded by the European Regional Development Fund (ERDF).

References

- [1] B. Glaubitz, S. Buschhorn, F. Brüssing, R. Abrudan, H. Zabel, *J. Phys. Condens. Matter* **23**, 25 (2011).
- [2] B.P. Weiss, J. Gattaccera, S. Stanley, P. Rochette, U.R. Christensen, *Space Sci. Rev.* **152**, 1 (2010).
- [3] M.W.R. Volk, M.R. Wack, B.J. Maier, *J. Alloys Compd.* **732**, 336 (2018).
- [4] Y. Geng, T. Ablekim, M. A. Koten, M. Weber, K. Lynn, J.E. Shield, *J. Alloys Compd.* **633**, 250 (2015).
- [5] J. Zhou, W. Yang, Ch. Yuan, B. Sun, B. Shen, *J. Alloys Compd.* **742**, 318 (2018).
- [6] D. Olešáková, P. Kollár, J. Füzér, *Acta Phys. Pol. A* **133**, 639 (2018).
- [7] M. Karolus, E. Jartych, D. Oleszak, *Acta Phys. Pol. A* **102**, 253 (2002).
- [8] C. Suryanarayana, *Prog. Mater. Sci.* **46**, 1 (2001).
- [9] P. Kollár, P. Slovenský, D. Olešáková, M. Jakubčín, Z. Birčáková, J. Füzér, R. Bureš, M. Fáberová, *J. Magn. Magn. Mater.* **494**, 165770 (2020).
- [10] W. Steinhaus, E. Gumlich, *Verhandl. Deut. Physik. Ges* **17**, 369 (1915).
- [11] M. Nowicki, *Materials* **11**(10), 1 (2018).
- [12] J. Pearson, P.T. Squire, D. Atkinson, *IEEE Trans. Magn.* **33**, 3970 (1997).
- [13] P. Kollár, Z. Birčáková, V. Vojtek, J. Füzér, R. Bureš, M. Fáberová, *J. Magn. Magn. Mater.* **388**, 76 (2015).
- [14] L. Novák, A. Lovaš, L.F. Kiss, *J. Appl. Phys.* **98**, 043904 (2005).
- [15] D.C. Jiles, D.L. Atherton, *J. Magn. Magn. Mater.* **61**, 48 (1986).
- [16] N.C. Pop, O.F. Calton, *Acta Phys. Pol. A* **120**, 491 (2011).
- [17] B. Kvasnica, F. Kundracík, *J. Magn. Magn. Mater.* **162**, 43 (1996).
- [18] Z. Birčáková, P. Kollár, J. Füzér, R. Bureš, M. Fáberová, *J. Magn. Magn. Mater.* **502**, 166514 (2020).